EUKARYOTIC CELL, Aug. 2010, p. 1283–1293 Vol. 9, No. 8
1535-9778/10/$12.00 doi:10.1128/EC.00015-10

Downregulation of an *Entamoeba histolytica* Rhomboid Protease Reveals Roles in Regulating Parasite Adhesion and Phagocytosis▽†

Leigh A. Baxt,[1] Elena Rastew,[1] Rivka Bracha,[2] David Mirelman,[2] and Upinder Singh[1,3]*

Department of Microbiology and Immunology, Stanford University School of Medicine, Stanford, California 94305[1]; Department of Biological Chemistry, Weizmann Institute of Science, Rehovot 76100, Israel[2]; and Department of Internal Medicine, Division of Infectious Diseases, Stanford University School of Medicine, 300 Pasteur Drive, Stanford, California 94305[3]

Received 19 January 2010/Accepted 11 June 2010

Entamoeba histolytica **is a deep-branching eukaryotic pathogen. Rhomboid proteases are intramembrane serine proteases, which cleave transmembrane proteins in, or in close proximity to, their transmembrane domain. We have previously shown that *E. histolytica* contains a single functional rhomboid protease (EhROM1) and has unique substrate specificity. EhROM1 is present on the trophozoite surface and relocalizes to internal vesicles during erythrophagocytosis and to the base of the cap during surface receptor capping. In order to further examine the biological function of EhROM1 we downregulated EhROM1 expression by >95% by utilizing the epigenetic silencing mechanism of the G3 parasite strain. Despite the observation that EhROM1 relocalized to the cap during surface receptor capping, EhROM1 knockdown [ROM(KD)] parasites had no gross changes in cap formation or complement resistance. However, ROM(KD) parasites demonstrated decreased host cell adhesion, a result recapitulated by treatment of wild-type parasites with DCI, a serine protease inhibitor with activity against rhomboid proteases. The reduced adhesion phenotype of ROM(KD) parasites was noted exclusively with healthy cells, and not with apoptotic cells. Additionally, ROM(KD) parasites had decreased phagocytic ability with reduced ingestion of healthy cells, apoptotic cells, and rice starch. Decreased phagocytic ability is thus independent of the reduced adhesion phenotype, since phagocytosis of apoptotic cells was reduced despite normal adhesion levels. The defect in host cell adhesion was not explained by altered expression or localization of the heavy subunit of the Gal/GalNAc surface lectin. These results suggest no significant role of EhROM1 in complement resistance but unexpected roles in parasite adhesion and phagocytosis.**

Entamoeba histolytica is an extracellular protozoan parasite and is a leading parasitic cause of death worldwide (48). The factors, which determine the outcome of amebic infection, are currently unknown, although it is likely that a combination of host and parasite determinants influence clinical outcome. A number of parasite factors required for amebic pathogenesis have been identified, including the Gal/GalNAc surface lectin, pore-forming proteins, and cysteine proteases (36–38, 41).

Recently, we identified several members of a class of intramembrane rhomboid proteases in the *E. histolytica* genome (4). Rhomboid proteases are seven-pass transmembrane proteases first identified in *Drosophila melanogaster* whose active site lies within the lipid bilayer, allowing them to cleave transmembrane proteins (6, 32). Substrates of rhomboid proteases are largely single-pass transmembrane proteins whose transmembrane domain contains helix-breaking residues (52). Recent work has revealed that there are multiple classes of rhomboid proteases that recognize different types of sequences within the transmembrane domains of their substrates (3). Despite low sequence similarity between individual rhomboid proteases of each class, these enzymes share a remarkable ability to functionally replace one another (16, 28, 52).

Rhomboid proteases have been studied in flies, bacteria, mammals, and parasites, and roles ranging from quorum sensing to host cell entry have been identified (3, 11, 25, 33, 35, 46, 47, 49, 54, 59). In apicomplexan parasites, such as *Plasmodium falciparum* and *Toxoplasma gondii*, it has been suggested that rhomboid proteases mediate cleavage of surface adhesin proteins to facilitate host cell entry (3, 11, 46, 47). The *E. histolytica* genome encodes four rhomboid-like genes, with only a single gene containing the necessary catalytic residues for proteolytic activity (4). This gene, EhROM1, is a functional protease with substrate specificity similar to the *P. falciparum* ROM4 (PfROM4) (3, 4). In trophozoites EhROM1 is localized to the parasite surface and relocalizes to internal vesicles during erythrophagocytosis and to the base of the cap during surface receptor capping. We have shown that the heavy subunit of the amebic surface Gal/GalNAc lectin (Hgl) is a substrate of EhROM1 *in vitro*. Mutational analyses using a COS cell cleavage assay demonstrated that the cleavage of Hgl requires the catalytic serine in EhROM1 as well as a helix-breaking glycine residue in the transmembrane domain of Hgl (4). These data indicate that EhROM1 is a functional rhomboid protease whose physiological substrate may be Hgl.

In order to further elucidate the biological function of

* Corresponding author. Mailing address: Department of Internal Medicine, Stanford University School of Medicine, S-143 Grant Building, 300 Pasteur Drive, Stanford, CA 94305. Phone: (650) 723-4045. Fax: (650) 724-3892. E-mail: usingh@stanford.edu.

† Supplemental material for this article may be found at http://ec.asm.org/.

▽ Published ahead of print on 25 June 2010.

EhROM1 we have utilized the epigenetic silencing mechanism of the *E. histolytica* G3 strain (8, 9). The mechanism of gene silencing in G3 ameba is not well understood. However, it is known that the silencing mechanism is epigenetically maintained, and epigenetic changes in the chromatin state of the silenced genes have been noted (22). G3 parasites transfected with a plasmid containing an upstream region of the 5′ end of EhROM showed almost complete downregulation of expression; we have named these parasites ROM(KD) for ROM knockdown. Phenotypes examined in ROM(KD) parasites included cap formation, complement resistance, adhesion, phagocytosis, hemolysis, and motility. We observed defects in both adhesion and phagocytosis in the ROM(KD) parasites compared to the parent G3 strain but no changes in cap formation or complement resistance. Importantly, the reduced phagocytosis phenotype appears independent of the reduced adhesion phenotype, implying that EhROM1 has distinct roles in both pathways.

MATERIALS AND METHODS

ROM-silencing plasmid construction. In order to construct the silencing plasmid for EhROM1, the first 538 bp from the 5′ end of the Eh*ROM1* gene were cloned into the plasmid vector psAP-2 (8, 9) downstream of the 5′ upstream segment (473 bp) of the Eh*Ap-A* gene by using a 5′ NcoI site and a 3′ BamHI site with the following primers: forward, 5′-TACGCCATGGATTCTCCACCACATAAC-3′; reverse, 5′-GCGGATCCCATCCCAAGTCTTAATTGCATTG-3′ (restriction sites are underlined).

Generation and maintenance of stable transfectants. G3 parasites were transfected using two different methods (8, 9, 43). For the SuperFect-based method, trophozoites were seeded into 25-mm petri dishes and allowed to grow for 24 h. On the day of transfection 20 μg plasmid DNA was incubated for 10 min with 20 μl SuperFect (Qiagen) in a total volume of 200 μl M199 medium (Gibco). Cells were washed once with M199 followed by addition of 2 ml M199 supplemented with 15% heat-inactivated bovine serum. The SuperFect-DNA mixture was added in drops across the petri dish, and the dishes were covered by parafilm to minimize oxygen exposure. Parasites were incubated at 37°C for 4 h, iced for 10 min to release parasites from the dish, and transferred to a 15-ml glass tube containing fresh TYI medium. Parasites were allowed to grow for 48 h after transfection before addition of drug selection. Parasites were selected at 1 μg/ml neomycin and increased to a final concentration of 2 μg/ml neomycin. For the electroporation-based method, trophozoites were electroporated with 100 μg plasmid DNA. Parasites were allowed to grow for 48 h before the addition of drug selection. Transfectants were selected at an initial concentration of 6 μg/ml neomycin. EhROM1 expression levels were tested using Northern blot analysis and reverse transcriptase PCR. Once EhROM1 downregulation was confirmed, the parasites were removed from drug selection, maintained under standard culture conditions, and tested monthly for maintenance of EhROM1 downregulation. All phenotypic analyses were done with parasite strains that had a >95% decrease in EhROM1 expression and that were not under drug selection.

Northern blot analysis. Northern blot analysis was done as previously published (30). Briefly, total RNA was isolated from parasites by phenol-chloroform extraction, the concentration was determined using a spectrophotometer, and 20 μg of each sample was resolved on a gel containing 1× morpholinepropanesulfonic acid, 1% agarose, and 6% formaldehyde. RNA was transferred to a Hybond N^+ (Amersham) nylon membrane and cross-linked using UV light. The blots were prehybridized in ExpressHyb hybridization buffer (Clontech) at 68°C for a minimum of 1 h. Double-stranded PCR probes were labeled with [α-^{32}P]dATP or [α-^{32}P]dCTP using Klenow (New England Biolabs) followed by hybridization of membranes at 68°C for approximately 18 h. Blots were washed as follows: the first wash was for 25 min in buffer containing 2× SSC (1× SSC is 0.15 M NaCl plus 0.015 M sodium citrate), 0.05% SDS, and the second wash was in buffer containing 0.1× SSC, 0.1% SDS. Blots were then exposed overnight to a Kodak phosphor screen at room temperature. Phosphor screens were scanned on a Bio-Rad phosphorimager.

Reverse transcriptase PCR. Reverse transcriptase PCR (RT-PCR) was performed by incubating approximately 2 μg total RNA with DNase for 15 min at 37°C. The reaction was stopped by addition of EDTA to a concentration of 2.5 mM followed by incubation at 65°C for 10 min. Following DNase treatment, the RNA was separated into two aliquots. One was kept on ice as a no-RT control, and the other was incubated with Superscript II reverse transcriptase (Invitrogen) and 10 mM deoxynucleoside triphosphates at 42°C for 2 h. Remaining RNA was hydrolyzed by addition of EDTA and NaOH and incubation at 70°C for 10 min. Samples (both with and without RT) were diluted in 500 μl Tris-EDTA buffer and passed through a YM-30 Microcon column (Millipore). One microliter of cDNA was then used as a template for PCRs of EhROM1, Hgl, Lgl-1, or single-stranded RNA (ssRNA). All PCRs were done for 35 cycles. Primers used were the following: EhROM1 (EHI_197460) F, 5′-AGGCCTTCATTCTCCACCACATAACAATA-3′, and R, 5′-GAGCTCTTAATTGCATTTTCCAACATTG-3′; Hgl (EHI_077500) F, 5′-ACTAGTTTATAAACTTCACTTACC-3′, and R, 5′-CCTAGGTCCATTGAATATTGCT-3′; Lgl-1 (EHI_035690) F, 5′-AGGCCTATGATTATATTAGTCTTATTGATA-3′, and R, 5′-GAGCTCTTATGCAAACACAGGAATAA-3′; ssRNA (X61116) F, 5′-ACGAACGAGACTGAAACCTAT-3′, and R, 5′-TGTTACGACTTCTCCTTCCTC-3′.

Complement resistance assays. To assay resistance of parasites to human complement, a previously published protocol was followed, with some modifications (20). Briefly, trophozoites were harvested and washed in phosphate-buffered saline (PBS) and brought to a concentration of 1.2×10^6 to 1.5×10^6/ml. A total of 60,000 to 70,000 trophozoites were incubated with 10% normal human serum (NHS) in buffer containing 1× PBS, 1.25 mM $MgCL_2$, 5 mM EGTA for 20 or 40 min at 37°C. As a control for cell viability, trophozoites were incubated with 10% heat-inactivated NHS for 40 min. Parasites were then stained with 0.2% trypan blue in PBS, followed by counting the total number of parasites and those which had excluded the dye. The average number of viable cells for the zero time point was set at 100%, and each subsequent time point was calculated as a percentage of the initial time point.

Hemolysis assay. Hemolysis of human red blood cells (HRBC) by intact trophozoites was performed as previously described (34). In brief, *E. histolytica* trophozoites were mixed with HRBC at a ratio of 1:2,000 trophozoites/HRBC (5×10^5 ameba/10^9 RBC) in 1 ml of hemolysis buffer [100 mM NaCl, 30 mM KCl, 100 mM sorbitol, 0.1% bovine serum albumin (BSA), and 10 mM piperazine-*N*,*N*′-bis(2-ethanesulfonic acid)-Tris (pH 6.8)]. The cell mixture was incubated for up to 90 min at 37°C. The tubes were then spun down ($1,000 \times g$ for 5 min), and the hemoglobin that was released into the supernatant was read at 570 nm. The background used was based on HRBC incubated in the absence of trophozoites.

Transwell motility assays. Transwell motility assays were performed according to previous methods (17). Briefly, parasites were grown to confluence in T25 flasks. Adherent cells were washed once with serum-free TYI medium. The medium was then replaced with serum-free TYI supplemented with 2 μg/ml 5-chloromethylfluorescein diacetate (CMFDA) cell tracker dye (Invitrogen). Flasks were covered in foil and incubated at 37°C for 1 h. After staining, parasites were removed from flasks by using a cell scraper and quantified with a hemacytometer. Cells were pelleted and resuspended in serum-free TYI at a concentration of 500,000 cells/ml, and 300 μl of this mixture (150,000 parasites) was added to the top of each 24-well transwell insert containing 8-μm pores (Costar). One milliliter of complete TYI-S-33 medium was placed in the bottom of the chamber. A control well with no insert but an equivalent number of parasites in 1 ml of complete TYI medium was used to normalize for potential differences in cell labeling. The 24-well plate was covered in foil and placed in an anaerobic bag for 4 h at 37°C, after which the transwells were removed and medium was aspirated and replaced with 1 ml of 1× PBS. Plates were read on a fluorescence plate reader at 492 nm (excitation) and 517 nm (emission).

Adherence assays. Adherence assays with healthy cells were performed using Chinese hamster ovary (CHO) cells according to previously described methods (30). Briefly, approximately 1×10^4 parasites plus 2×10^5 CHO cells were mixed together in M199 (supplemented with 25 mM HEPES [pH 6.8], 5.7 mM cysteine, 0.5% BSA, 10% heat-inactivated bovine serum). This mixture was centrifuged at $150 \times g$ for 5 min and incubated on ice for 2 h. After incubation, tubes were vortexed briefly and a hemocytometer was used to count the parasites with CHO cells attached. Parasites with three or more cells attached were considered positive for adhesion. To test the effect of 3,4-dichloroisocoumarin (DCI) on parasite adhesion, 100 μM DCI (Sigma-Aldrich) was dissolved in dimethl sulfoxide (DMSO) and applied to the parasites for 2 h during the incubation. Control parasites were treated with DMSO alone.

Apoptotic CHO cells were generated using staurosporine aglycone, an established inducer of apoptosis (5, 44). Prior to use, CHO cultures were enriched for viable cells by centrifugation at 600 rpm for 10 min at room temperature by applying Ficoll-Paque Plus (GE Healthcare). Viable cells were collected on top of the Ficoll-Paque layer and split into two groups. In one group apoptosis was induced by treatment with 100 μM staurosporine aglycone (Sigma-Aldrich; dis-

solved in DMSO) for 1 h at 4°C. Alternatively, control parasites were treated with 100 μM DMSO.

Induction of capping and indirect immunofluorescence assays. Capping was induced according to previous methods (1). Briefly, parasites were seeded into chamber slides (LabTek) and allowed to adhere at 37°C for 30 min. Parasites were rinsed once in 1× PBS (minue $CaCl_2$). Then, 250 μl 1× PBS with 20 μg/ml concanavalin A (biotin labeled) was added to each chamber, and parasites were incubated on ice for 1 h. After incubation on ice 750 μl of prewarmed 1× PBS was added to each well, the wells were covered with parafilm, and slides were placed in a 37°C water bath for 20 min to induce cap formation. Buffer was subsequently removed, and parasites were fixed with 4% ultrapure formaldehyde diluted in PBS plus 10 mM $MgCl_2$ for 12 min. Cells were permeabilized by addition of 100% ethanol (EtOH) for 20 min followed by blocking in 3% BSA–PBS for 30 min. Cells were stained with primary antibody diluted in 1% BSA–PBS and incubated at room temperature for 1 h, followed by staining with fluorescent secondary antibodies in the dark for 1 h at room temperature. Antibody dilutions were as follows: anti-Hgl (mouse monoclonal antibody 3F4 and 7F4 together; each at 1:30) and anti-EhROM1 (rat polyclonal; 1:20), streptavidin Texas Red (1:500), Alexa 488 goat anti-mouse (1:1,000), or Alexa 488 goat anti-rat secondary antibody (1:1,000). Imaging was performed on a Leica CTR6000 microscope, using a BD CARVII confocal unit. Image analysis and deconvolution were performed using the LAS-AF program from Leica. Deconvolution was performed in 10 iterations with a single deconvolved slice shown for each sample.

Phagocytosis assays. Erythrophagocytosis was analyzed as previously published (34). Briefly, 5×10^7 HRBC were incubated with 5×10^5 trophozoites in 1 ml PBS for 15 min at 37°C. The extracellular RBC were lysed by adding ice-cold distilled water and spinning the suspension twice. Pellets containing parasites and ingested HRBC were lysed in concentrated formic acid (90%), and solutions were read on a spectrophotometer at 397 nm.

Ingestion of starch was assayed by microscopy. Trophozoites (1×10^5) were seeded into 12-well cell culture plates (Cellstar) and allowed to adhere for 2 h at 37°C. TYI-S-33 medium containing approximately 0.004% rice starch (MP Biomedicals) was added and incubated at 37°C for 1 h. This was followed by three PBS washes, fixation in 100% EtOH for 20 min, and staining with 1% (vol/vol) Lugol's solution at room temperature for 5 min. Rice starch stained dark brown, and parasites with one or more ingested starch grains were considered positive for rice starch phagocytosis. A minimum of 100 parasites were counted for each treatment, and the experiment was repeated a minimum of three times.

Phagocytosis of CHO cells was performed as follows. Prior to use, CHO cultures were enriched for viable cells by applying the Ficoll-Paque Plus method as previously outlined. A total of 0.5×10^5 CHO cells were treated under apoptosis-inducing conditions (100 μM staurosporine) or as controls (100 μM DMSO) for 1 h at 4°C and added to parasites (1:1 ratio) by spinning at 200 rpm for 5 min. Parasite-CHO cells were incubated for 15 min at 37°C, fixed with 4% formaldehyde for 12 min, permeabilized in 100% EtOH for 20 min, and stained with 1% (vol/vol) trichrome stain. Parasites with one or more ingested CHO cells were considered positive for phagocytosis. A minimum of 50 parasites were counted for each treatment, and the experiment was repeated a minimum of three times.

Western blot analysis. Lysates were prepared using log-phase trophozoites. Trophozoites were iced for 10 min and pelleted at $1{,}000 \times g$ for 5 min at 4°C, followed by a single wash in ice-cold 1× PBS. Parasites were resuspended in lysis buffer (50 mM HEPES-KOH [pH 7.5], 50 mM KCl, 5 mM $MgCl_2$, 0.5% NP-40) containing protease inhibitors (2 mM dithiothreitol, 375 μM E-64, 0.4 μg/ml leupeptin, 1× HALT inhibitor cocktail [catalog no. 78410; Thermo Scientific]), and then incubated on ice, and a Bradford assay was used to determine protein concentrations. Lysates were run on a standard 8 to 10% SDS-PAGE gel and transferred overnight at 35 mA at 4°C to a polyvinylidene difluoride membrane. The membrane was blocked with 5% milk in PBS–0.1% Tween 20 for a minimum of 1 h. Blots were then incubated with antibodies to Hgl (H85; 1:50), pan-actin (1:250; Cell Signaling), or anti-EhROM1 (1:1,000), diluted in 5% milk– PBS–0.1% Tween 20 overnight at 4°C followed by incubation with secondary horseradish peroxidase (HRP)-conjugated antibodies diluted in the same solution (1:1,000 or 1:5,000) and developed using enhanced chemiluminescence (ECL). Blots were scanned on a Kodak Image Station 4000R.

***E. histolytica* Gal/GalNAc lectin ELISA.** For quantification of *E. histolytica* lectin present in the whole amebic cell lysates as well as in conditioned TYI-S-33 serum-free medium, an *E. histolytica* II lectin enzyme immunoassay (Techlab) was performed according to the manufacturer's instructions. Briefly, amebic lysates were prepared as described for Western blotting and adjusted to 50 ng of total protein. Conditioned medium was prepared by growing log-phase trophozoites in serum-free medium for 24 h. Medium was collected and centrifuged at $1{,}000 \times g$ for 5 min at 4°C to pellet intact amebas and further subjected to ultracentrifugation at $210{,}000 \times g$ for 30 min at 4°C. Prior to use the total medium protein concentration was adjusted to 400 ng. The microassay plate was coated with monoclonal antibody specific for *E. histolytica* lectin and incubated directly with a sample. An internal sample of purified *E. histolytica* lectin was used as a positive control, and assay diluent was the negative control. After washing five times, the enzyme-linked immunosorbent assay (ELISA) was developed by adding the substrate to the plate followed by the stop solution. The amebic lectin was quantified by measuring the optical density at 450 nm on a microplate ELISA reader. The experiment was performed three times, and results were averaged.

Microarray analysis of ROM(KD) parasites. To identify potential changes in gene expression of the Gal/GalNAc lectin due to ROM1 silencing, total RNA from G3 or ROM(KD) parasites was isolated with Trizol reagent (Invitrogen) using standard protocols (29). The RNA samples were further cleaned with the RNeasy kit (Qiagen) before being used for microarray analysis. Samples were processed for microarray hybridization by the Stanford University Protein and Nucleic Acids facility (http://cmgm.stanford.edu/pan/) using standard protocols. For each sample the RNA quality was checked using an Agilent BioAnalyser QC. RNA samples (4 mg) were labeled and hybridized to a custom Affymetrix array full-genome microarray (18) using standard protocols. Raw probe intensities generated by using the GCOS software (Affymetrix) were processed with R 2.2.0 using robust multiarray averaging with correction for oligo sequence (gcRMA), downloaded from the BioConductor project (http://www.bioconductor.org). Two independent biological samples of G3 and ROM(KD) parasites were analyzed. Genes annotated as Gal/GalNAc lectin (heavy and light subunits) and rhomboid protease (EhROM1 to -4) were analyzed for expression levels. A control gene, actin (EHI_163580), was also analyzed. Results of the microarray were confirmed by semiquantitative RT-PCR using the methods outlined above.

Microarray data accession number. The microarray data for gene expression of G3 and ROM(KD) parasites were deposited in the GEO database (http://www.ncbi.nlm.nih.gov/geo/query/acc.cgi?acc=GSE21522) under the accession number GSE 21522 and NCBI tracking system number 15843481.

RESULTS

Downregulation of EhROM1 in *E. histolytica* G3 strain. In order to elucidate the function of EhROM1 we sought to downregulate its expression. We utilized a number of approaches, including dsRNA expression, inducible expression of antisense transcript, and constitutive expression of antisense transcript, but were unable to significantly downregulate expression of EhROM1 using any of these methods (data not shown). We also generated an EhROM1 serine to alanine (S→A) catalytic mutant, which may function in a dominant negative fashion. However, this construct did not target appropriately to the parasite surface (data not shown). In our experience both N- and C-terminally tagged EhROM1 fusion proteins did not localize to the parasite surface, regardless of the use of a small (Myc) or large (green fluorescent protein) tag (data not shown). Therefore, any phenotype due to the presence of EhROM1 on the parasite surface would be difficult to assess using a tagged EhROM1 S-A catalytic mutant.

Thus, we chose to use the epigenetic silencing mechanism utilizing the *E. histolytica* G3 line of parasites (8, 9, 12). We utilized a plasmid containing the Eh*Ap-A* 5′ upstream region cloned upstream of the first 538 bp from the 5′ end of Eh*ROM1* (Fig. 1A). We generated stable transfectants in drug selection for approximately 1 month and examined expression of EhROM1. Two independent lines of transfectants with downregulation of EhROM1 were generated; one line was generated by electroporation in the Mirelman lab and another line was generated by lipid-based transfection in the Singh lab. Transfectants from both labs were maintained with drug selection for at least 1 month prior to removal of drug selection. Parasites were cured of plasmid in order to avoid any second-

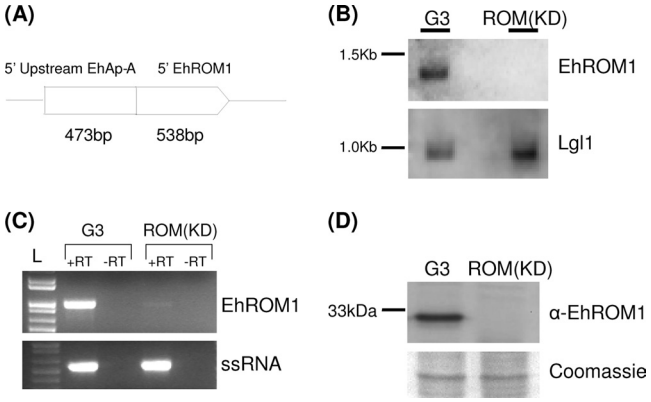

FIG. 1. The G3-based approach downregulates expression of EhROM1. (A) Schematic of the G3 EhROM1 silencing construct used in our studies. A 538-bp 5′ region of Eh*ROM1* was fused downstream of the Eh*Ap-A* cassette. (B) Northern blot analysis of EhROM1 expression in G3 and ROM(KD) parasites. Twenty micrograms of total RNA was resolved on an a formaldehyde gel and probed sequentially with probes for EhROM1 and Lgl1, which served as a loading control. (C) RT-PCR analysis of EhROM1 expression levels in G3 and ROM(KD) parasites. One-microgram aliquots of cDNA from G3 and ROM(KD) cell lines were subjected to 35 cycles of PCR for EhROM1; ssRNA was used as a loading control. PCR from samples without RT served as controls to exclude genomic DNA contamination. (D) Western blot analysis of EhROM1 in G3 and ROM(KD) parasites. Parasite lysates were resolved on a 10% SDS-PAGE gel and probed with anti-EhROM1 antibody (1:1,000), detected with HRP-conjugated secondary antibody (1:5,000), and developed using ECL. Blots were scanned on a Kodak Image Station 4000R.

ary phenotypic effects caused by drug selection. Transfectants in the Mirelman lab were cloned from a single parasite, while those in the Singh lab were maintained as a heterogeneous population. Both lines of parasites were assayed by Northern blotting, RT-PCR, and Western blotting for expression of EhROM1 transcript and protein, respectively. For both transfectant parasite lines, expression of EhROM1 transcript was undetectable by Northern blotting (Fig. 1B), while RT-PCR revealed a small amount (<5%) of EhROM1 transcript present (Fig. 1C). Western blot assays revealed no signal from an EhROM1-specific antibody (Fig. 1D). Thus, both lines of transfectants were named ROM(KD), as they exhibited greater than 95% knockdown of EhROM1 expression at the RNA and protein levels. Representative data from transfectants in the Mirelman lab (Fig. 1D) and Singh lab (Fig. 1B and C) are shown. Additionally, our microarray data confirmed the downregulation of EhROM1 expression by 479-fold in ROM(KD) parasites compared to G3 (Table 1). Expression levels of other ROMs were not significantly changed.

ROM(KD) parasites are not altered in cap formation. Our previous data indicated that the heavy subunit of the Gal/GalNAc lectin, Hgl, is a substrate of EhROM1 *in vitro* (4). In order to study the biological function of potential Hgl cleavage by EhROM1 in trophozoites, we selected a wide range of phenotypic assays to examine in ROM(KD) parasites. Phenotypes examined included surface receptor capping, localization of Hgl to caps, complement resistance, adhesion, phagocytosis, and motility. For all assays we compared ROM(KD) parasites removed from neomycin selection to G3 parasites in order to avoid any secondary effects of drug selection.

E. histolytica employs a number of strategies to avoid lysis by the host complement system (13, 15, 21, 39, 40, 45). Surface receptor capping is one mechanism that is induced by the presence of antibodies directed against parasite surface proteins. Binding of antibodies to surface receptors on the parasite results in the polarization of these receptors to the posterior end, where they form a cap (13, 14, 45). The cap is subsequently released from the parasite (through an unknown mechanism), allowing the parasite to evade the host immune system. Other mechanisms of complement resistance in *E. histolytica* include cleavage of components of the membrane attack complex by parasite proteases and homology between human CD59 and the heavy subunit of the amebic lectin, which prevents assembly of the membrane attack complex on the parasite surface (10, 39, 40). We have shown previously that EhROM1 relocalizes to the base of the caps formed during surface receptor capping (4). The amebic Gal/GalNAc lectin is known to elicit a robust antibody response in the host and is thus one of the proteins targeted to the cap for release (13–15). Our previous work identified the heavy subunit of this lectin as a substrate of EhROM1 *in vitro* (4). In order to determine whether the relocalization of EhROM1 to the base of the cap indicates that it plays a role in cap formation, release, or cleavage of Hgl we examined cap formation, localization of Hgl to the cap, and complement resistance in ROM(KD) parasites.

Capping was induced *in vitro* by incubating parasites with a synthetic lectin, concanavalin A (ConA), followed by incubating parasites at 37°C for 15 min. Parasites were fixed and stained to allow visualization of the ConA (which has a biotin tag) and either Hgl or EhROM1. We observed the formation of morphologically indistinguishable caps in both G3 and ROM(KD) parasites (Fig. 2A and B). ROM(KD) parasites showed low signal with the EhROM1 antibody, as expected (Fig. 2A). Caps in both ROM(KD) and G3 parasites showed dramatic enrichment of Hgl (Fig. 2B).

ROM(KD) parasites displayed no change in complement resistance or motility. In order to examine a biologically relevant phenotype associated with capping, we examined the ability of ROM(KD) parasites to resist lysis by human complement. Complement resistance was measured by incubating G3 or ROM(KD) parasites with human serum for 20 or 40 min followed by trypan blue staining to assess parasite viability. No

TABLE 1. Expression levels of selected genes in G3 and ROM(KD) parasites

Gene name (EHI no.)	Expression level (avg ± SD) in:		Fold change [G3 vs ROM(KD)]
	G3	ROM(KD)	
ROM1 (EHI_197460)	33 ± 6.85	0.07 ± 0.22	479
ROM2 (EHI_060330)	0.33 ± 0.14	0.29 ± 0.54	1.14
ROM3 (EHI_029220)	1.65 ± 0.15	1.56 ± 0.10	1.06
ROM4 (EHI_128190)	0.93 ± 0.33	0.78 ± 0.16	1.19
Hgl (EHI_046650)	6.39 ± 3.33	7.46 ± 0.49	0.85
Hgl (no EHI no.)	89.8 ± 0.97	86.08 ± 0.57	1.04
Igl (EHI_006980)	53.7 ± 9.88	40.23 ± 0.94	1.35
Igl (EHI_148790)	14.49 ± 0.03	12.28 ± 0.97	1.18
Lgl (EHI_058330)	2.86 ± 0.18	3.88 ± 0.36	0.73
Lgl (EHI_035690)	176.1 ± 0.26	177.3 ± 5.3	0.99
Actin (EHI_163580)	13.9 ± 0.34	14.6 ± 0.29	0.95

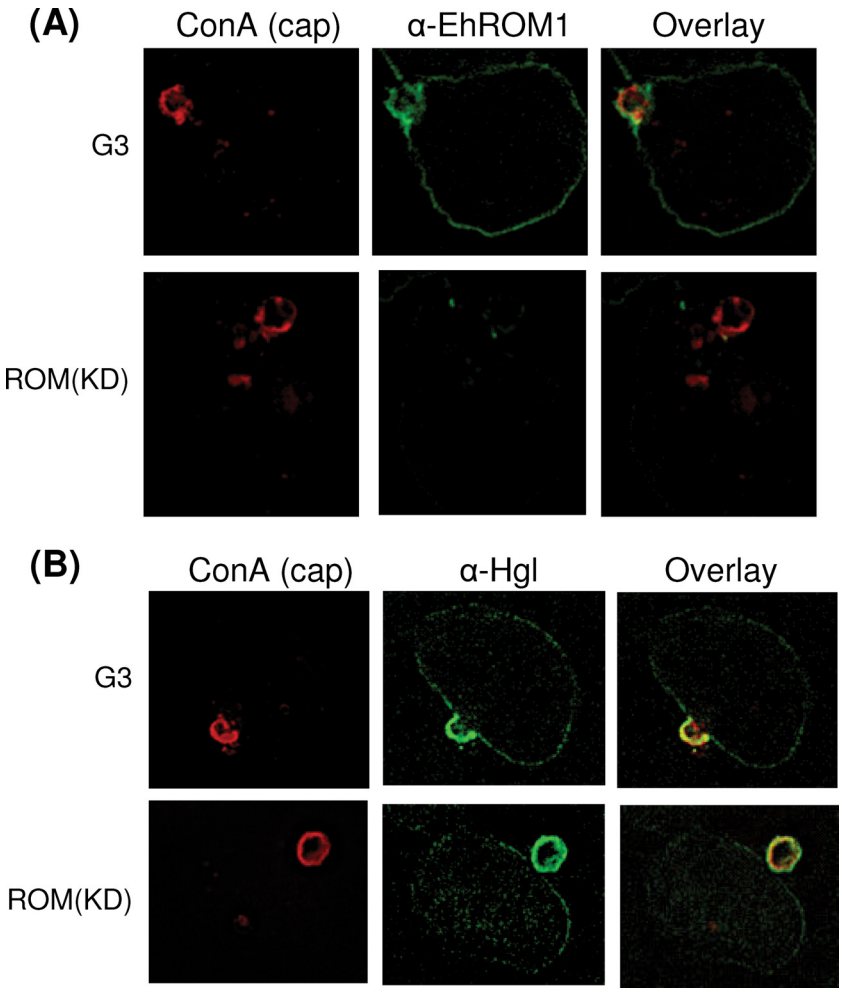

FIG. 2. ROM(KD) parasites form caps that are morphologically indistinguishable from G3 parasites. Capping was induced in G3 and ROM(KD) parasites *in vitro* by incubation of parasites with ConA on ice followed by incubation at 37°C for 15 min. Parasites were then fixed and stained with anti-EhROM1 (1:20) (A) or anti-Hgl (3F4 [1:30] plus 7F4 [1:30] antibodies) (B) followed by incubation with fluorescent secondary antibodies. Parasites were stained with Texas Red-streptavidin (1:500) in order to image caps (ConA contains a biotin tag). All imaging was performed on a Leica CTR6000 microscope, using a BD CARVII confocal unit. Image analysis and deconvolution were performed using the LAS-AF program from Leica. Deconvolution was performed in 10 iterations, with a single deconvolved slice shown for each sample.

change in complement resistance was observed in ROM(KD) parasites compared to G3 (Fig. 3A). Between 60 and 70% of parasites were killed after a 20-min incubation with serum, and between 70 and 80% were killed after 40 min. These data indicate that ROM(KD) parasites exhibit no change in cap formation or complement resistance.

Parasite motility is a key virulence factor, as it is required for multiple steps of the invasion process (27, 57). Parasites must maneuver across the colonic epithelium, penetrate the destroyed epithelial barrier, and travel to extraintestinal sites of infection. Due to the localization of EhROM1 to the parasite surface and the potential for this protease to cleave surface adhesins, we decided to investigate any changes in amebic motility associated with downregulation of EhROM1 expression. A transwell assay has been developed to measure motility in *E. histolytica* (17). Parasites are labeled with a fluorescent cell tracking dye, CMFDA, and placed in the top chamber of a transwell system resuspended in serum-free medium. The bottom chamber below the transwell is filled with serum-containing medium in order to induce parasite migration from the upper chamber to the lower chamber. Pores in the transwell are smaller than parasites and thus parasites must use active motility to migrate through these pores. We performed transwell motility assays in parallel for G3 and ROM(KD) parasites and observed no change in transwell migration between these parasite lines (Fig. 3B). Despite many studies demonstrating their cleavage of parasite surface adhesins, rhomboid proteases have not been implicated in parasite motility (3, 11, 47). Disruption of *Plasmodium berghei* ROM1 did not affect sporozoite gliding motility, suggesting that surface proteins involved in this type of motility are not rhomboid substrates (47).

ROM(KD) parasites have a defect in adherence to healthy host cells. Adhesion to host cells is a crucial step in the pathogenesis of *E. histolytica*. Binding of the parasite Gal/GalNAc lectin to host cells is a required step for the induction of apoptosis in host cells and cytotoxicity (24, 36, 42). We have shown previously that EhROM1 is localized to the surface of trophozoites; thus, it could potentially play a role in regulating

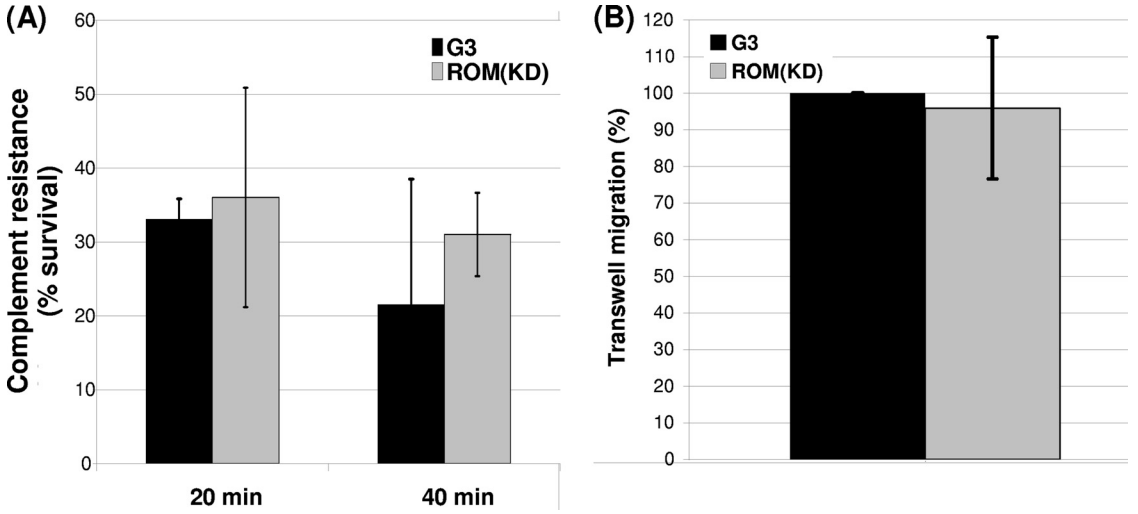

FIG. 3. Complement resistance and motility are not significantly altered in ROM(KD) parasites. (A) Complement resistance was measured by incubation of trophozoites with 10% NHS for 20 or 40 min at 37°C. Following incubation with complement, parasites were stained with 0.2% trypan blue to assess cell viability. The averages of two experiments, each with a single replicate, are shown with standard deviations. (B) Motility was measured by fluorescently labeling parasites with the cell tracker dye CMFDA. Parasites were added to the upper chamber of a transwell system in serum-free medium and allowed to migrate into the lower chamber containing complete medium for 4 h at 37°C. After incubation parasites in the lower chamber were quantified by reading on a fluorescence plate reader. The averages of three independent experiments, each with three replicates, are shown with standard deviations. Data are shown as the percentage of G3 motility.

parasite adhesion (4). In order to investigate this possibility we measured the abilities of both G3 and ROM(KD) parasites to adhere to healthy (untreated) CHO cells in a standard CHO cell rosette assay (30). Adhesion assays comparing G3 and ROM(KD) parasites showed a consistent ~35% decrease in adhesion by ROM(KD) compared to G3 parasites ($P < 0.001$) (Fig. 4A).

In order to corroborate the adhesion phenotype with another assay in which EhROM1 is inhibited, we examined the effect of rhomboid protease inhibitors on parasite adhesion to host cells. It has been demonstrated that isocoumarin compounds, including DCI, inhibit rhomboid proteases by alkylating the histidine, whereas compounds directed against the serine nucleophile (such as phenylmethylsulfonyl fluoride [PMSF]) did not have any significant effect on substrate cleavage by rhomboid proteases (55). We tested the effect of DCI on *E. histolytica* HM-1:IMSS trophozoites and identified that in the presence of 100 μM DCI, parasites had an ~60% decrease in adhesion compared to controls (DMSO or PMSF) (Fig. 4B). These results were achieved with the wild-type *E.*

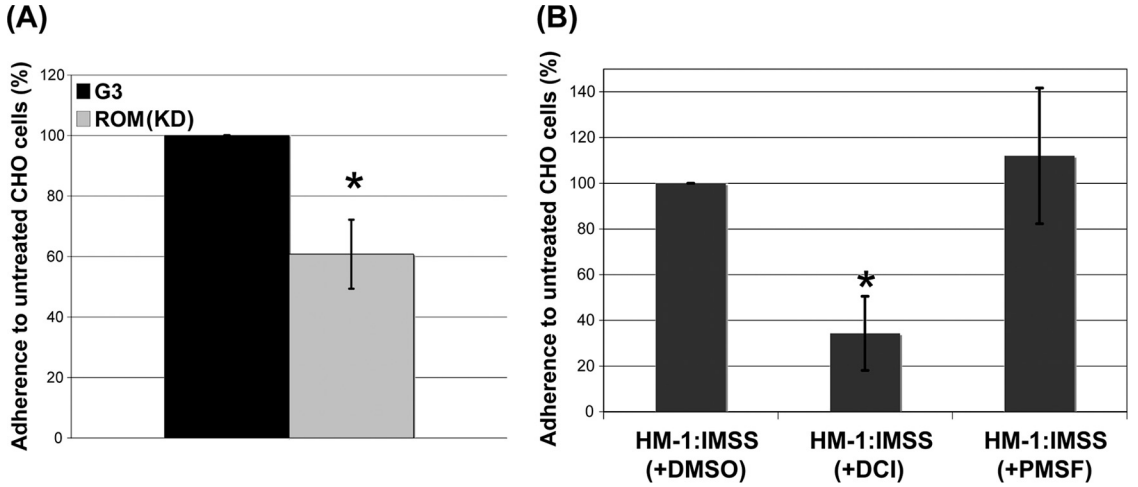

FIG. 4. Rhomboid protease inhibition results in a defect in adhesion to untreated CHO cells. (A) Adhesion was measured with a CHO cell rosette assay for G3 and ROM(KD) parasites. Parasites were mixed with CHO cells at 4°C for 2 h, after which parasites with three or more CHO cells attached were counted as positive. Data shown are an average of six experiments, each with two replicates. Standard deviations are shown. *, $P < 0.001$. (B) Adhesion for HM-1:IMSS parasites. The CHO cell rosette assay was modified by applying 100 μM DMSO (mock control),100 μM DCI (a serine protease inhibitor with activity for rhomboid proteases), or 100 μM PMSF (a serine protease inhibitor with no activity against rhomboid proteases) during the parasite-CHO cell 2-h incubation. Data shown are averages of two or three independent experiments, each with two replicates. Standard deviations are shown. *, $P < 0.002$.

histolytica HM-1:IMSS strain but also recapitulated with the G3 strain (data not shown). Since DCI, an inhibitor of rhomboid proteases, recapitulates the ROM(KD) adhesion defect (in both wild-type HM-1:IMSS and G3 strains), we propose that these data are consistent with a role in parasite adhesion for EhROM1. However, since DCI may have other unknown effects on *E. histolytica* trophozoites, the ROM(KD) strain is still the best way to specifically assess the function of EhROM1 in amebic trophozoites.

No significant changes in RNA or protein levels of Gal/GalNAc lectin were noted in the ROM(KD) parasites. The Gal/GalNAc lectin is one of the primary receptors known to be involved in mediating trophozoite adhesion (38, 42). In order to better understand the adhesion defect of ROM(KD) parasites, we investigated whether there were any potential changes in expression or the subcellular localization of Hgl. We observed no alterations in expression levels of the heavy subunit of the Gal/GalNAc lectin by microarray analysis (Table 1; see Table S1 in the supplemental material), RT-PCR (Fig. 5A), Western blotting (Fig. 5B), or ELISA (Fig. 5C and D). All techniques revealed that there were no major changes in expression or protein levels of either Hgl or Lgl-1 in ROM(KD) compared to G3 parasites. Additionally, no significant changes of lectin levels in amebic lysates or in conditioned media were noted as measured by an Hgl ELISA (Fig. 5C and D). We next examined whether any changes in the subcellular localization of Hgl could explain the defect we observed in adhesion of ROM(KD) parasites to CHO cells. Immunofluorescence imaging revealed no dramatic difference in surface or internal Hgl localization between G3 and ROM(KD) parasites in permeabilized or nonpermeabilized samples, respectively (Fig. 5E). Taken together, the adhesion defect of ROM(KD) parasites cannot be attributed to any changes in expression or localization of the amebic surface lectin.

ROM(KD) parasites have a decreased phagocytic ability compared to G3 parasites. Erythrophagocytosis is one indicator of amebic virulence potential. Pathogenic *E. histolytica* ingests erythrocytes, while nonpathogenic species such as *Entamoeba dispar* do not, a difference which has historically been used to diagnose with which species of *Entamoeba* an individual has been infected (51). Attachment to erythrocytes has been shown to be mediated by both the amebic Gal/GalNAc lectin as well as a transmembrane kinase (7, 36, 56). We have previously shown that EhROM1 localizes to phagocytic vesicles during erythrophagocytosis, suggesting that it could play a role in this process. We measured erythrophagocytosis in G3 and ROM(KD) parasites using a colorimetric assay; parasites were incubated with erythrocytes, extracellular erythrocytes were lysed in distilled water, and parasites containing ingested erythrocytes were lysed in concentrated formic acid. The resulting solution was measured with a spectrophotometer in order to quantify ingested erythrocytes. We compared the ability of G3 and ROM(KD) parasites to ingest human erythrocytes and observed a defect in erythrophagocytosis in ROM(KD) parasites compared to G3 ($P < 0.001$) (Fig. 6A). In both G3 and ROM(KD) parasites the addition of galactose (but not glucose) significantly inhibited (>60%) the rates of erythrophagocytosis, which confirms the role of the Gal/GalNAc lectin in erythrophagocytosis in these parasite strains (data not shown). It is noteworthy that no difference was detected in the hemolytic activity between G3 and ROM(KD) trophozoites (data not shown).

In order to investigate the role of EhROM1 during phagocytosis of another substrate, we compared the ability of ROM(KD) and G3 parasites to ingest rice starch. We considered parasites that had ingested at least one starch grain as actively phagocytic. Phagocytosis of rice starch was decreased by 25% in ROM(KD) compared to G3 ($P < 0.006$) (Fig. 6B). Thus, ROM(KD) parasites have a general decrease in their phagocytic ability.

ROM(KD) parasites have normal adherence to but decreased phagocytosis of apoptotic cells. There appear to be distinct receptors for amebic adhesion to healthy and apoptotic cells. The Gal/GalNAc lectin is involved in adhesion to healthy cells (38, 42). The phagosome-associated transmembrane kinase (PATMK) was shown to play a role in adhesion to both healthy and dying erythrocytes (7). Additionally, an immunogenic surface protein, the serine-rich *E. histolytica* protein (SREHP) identified in a screen for antibodies that blocked adhesion of trophozoites to apoptotic cells was shown to be the major receptor utilized by parasites during adhesion to apoptotic cells (50). Therefore, assaying the ability of ROM(KD) parasites to adhere to both healthy and apoptotic cells would help to further define whether the adhesion defect of ROM(KD) was due solely to the Gal/GalNAc lectin.

In order to determine whether ROM(KD) parasites had differential adherence to healthy and apoptotic cells, we measured adherence to healthy and staurosporine-treated cells. Staurosporine treatment consistently resulted in greater than 70 to 85% apoptotic cells, as determined by the presence of phosphatidylserine on the outer leaflet of the CHO cell plasma membrane, as measured by the BD Pharmingen Annexin V-fluorescein isothiocyanate fluorescence microscopy kit (data not shown). The adherence of G3 parasites to staurosporine-treated CHO cells was significantly diminished compared to DMSO-treated CHO cells ($P < 0.002$). This is consistent with previous studies, which demonstrated decreased adherence of apoptotic cells to amebic trophozoites (23). ROM(KD) parasites incubated with DMSO-treated CHO cells had a consistent ~25% decrease in adhesion compared to G3 parasites (Fig. 7A), similar to the adhesion defect of ROM(KD) to healthy nontreated CHO cells (Fig. 4A). The adherence of ROM(KD) parasites to staurosporine-treated CHO cells was less affected and was comparable to that of the G3 parasite (although significantly decreased compared to DMSO controls; $P < 0.003$) (Fig. 7A).

Next we assessed the ability of G3 and ROM(KD) parasites to phagocytose apoptotic CHO cells. It has previously been reported that phosphatidylserine exposure (as occurs in apoptotic cells) enhances *E. histolytica* engulfment of host cells (2, 23). We observed a similar phenomenon; G3 parasites had relatively increased ingestion of apoptotic cells compared to control (DMSO-treated) cells, once its reduced adherence defect was taken into account (Fig. 7). However, ROM(KD) parasites had significantly reduced phagocytosis of apoptotic cells, despite adhering to apoptotic cells at levels comparable to G3 parasites (Fig. 7B) ($P < 0.007$). These data implicate ROM(KD) parasites as having two independent phenotypes: decreased adherence and decreased phagocytosis.

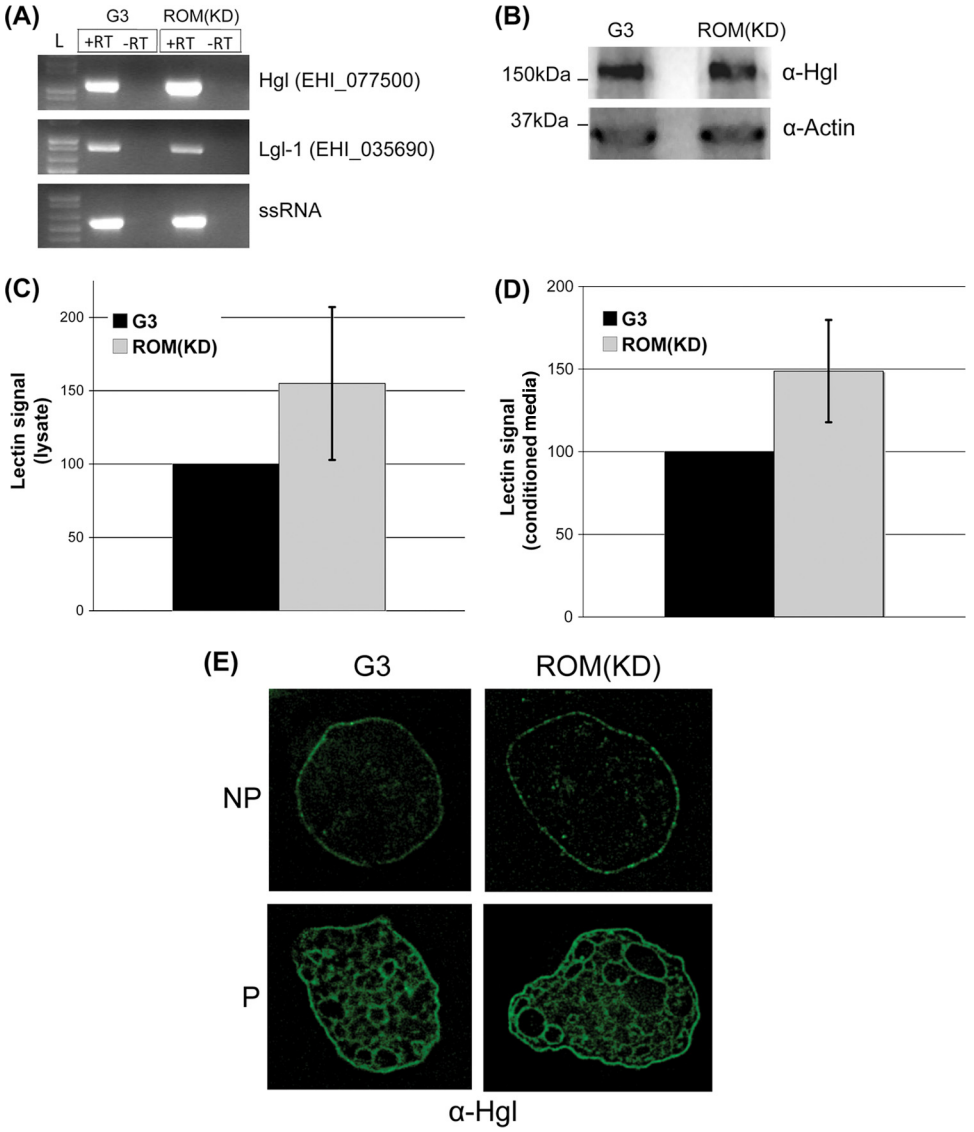

FIG. 5. No significant changes in expression, protein levels, or localization of the Gal/GalNAc lectin were noted in the ROM(KD) parasites. (A) Expression levels of Hgl and Lgl-1 transcripts were assayed by RT-PCR and matched the array data (Table 1); ssRNA was used as a control. Microarray data have been deposited at NCBI (see Materials and Methods). (B) Hgl protein expression was measured by Western blot analysis. Blots were probed with antibodies to Hgl (H85; 1:50) or actin (1:250) as a loading control. Western blot detection was performed using ECL. (C) ELISA measurement of *E. histolytica* lectin from the whole-cell lysates of G3 and ROM(KD) parasites. The parasites were lysed, and the final protein concentration was adjusted to 50 ng. The amount of lectin was quantified by measuring the optical density at 450 nm. (D) ELISA measurement of *E. histolytica* lectin from conditioned medium of G3 or ROM(KD) parasites, which was prepared by growing log-phase trophozoites in serum-free medium for 24 h. The protein concentration was adjusted to 400 ng, and lectin was quantitated using the manufacturer's instructions. Data shown are averages of three independent experiments with standard deviations. (E) Subcellular localization of Hgl was analyzed by staining both permeabilized (P) and nonpermeabilized (NP) parasites with anti-Hgl antibodies (3F4 [1:30] plus 7F4 [1:30]). All imaging was performed on a Leica CTR6000 microscope, using a BD CARVII confocal unit. Image analysis and deconvolution were performed using the LAS-AF program from Leica. Deconvolution was performed in 10 iterations, with a single deconvolved slice shown for each sample.

DISCUSSION

We downregulated expression of EhROM1 by utilizing the epigenetic method in *E. histolytica* G3 parasites (8, 9, 12). Phenotypes associated with amebic pathogenesis were examined in these parasites. These assays were selected based on the premise that Hgl, the heavy subunit of the Gal/GalNAc lectin and a major virulence determinant in *E. histolytica*, may be a substrate of EhROM1 (4). Additionally, phenotypes were analyzed based on presence of EhROM1 on the parasite surface and relocalization of EhROM1 to internal vesicles during erythrophagocytosis and to the base of caps during surface receptor capping (4). We demonstrated that ROM(KD) parasites had defects in adhesion to healthy cells, whereas adhesion to apoptotic cells was comparable to levels seen in the parent G3 strain. A generalized phagocytosis defect was noted in ROM(KD) parasites, with

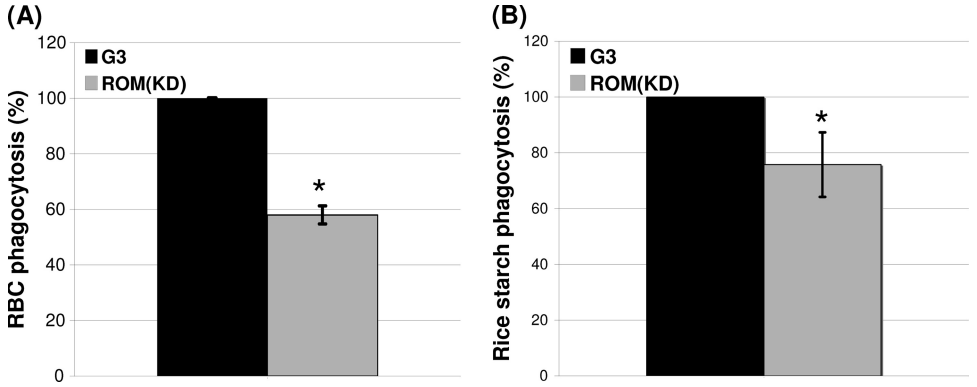

FIG. 6. ROM(KD) parasites show a defect in phagocytosis of red blood cells and rice starch. (A) A total of 5×10^7 HRBC were incubated with 5×10^5 trophozoites in a ratio of 100:1 in PBS for 15 min at 37°C, followed by lysis of extracellular RBC and measurement of ingested erythrocytes by lysis in 90% formic acid, followed by spectrophotometric determinations at 397 nm. The results represent the means and standard deviations of four independent experiments and are expressed as a percentage of the parent G3 strain erythrophagocytosis level. *, $P < 0.001$. (B) A total of 1×10^5 trophozoites were incubated for 1 h with 0.004% rice starch solution followed by fixation, permeabilization, and staining with 1% Lugol's solution at room temperature for 5 min. Parasites with one or more ingested starch grains were considered positive for rice starch phagocytosis. Data are averages of three independent experiments with standard deviations. *, $P < 0.006$.

reduced phagocytosis of erythrocytes and rice starch. Additionally, despite adhering to apoptotic cells at levels comparable to the G3 strain, ROM(KD) parasites had decreased phagocytosis of apoptotic cells. Taken together, the data indicate that the reduced adhesion and phagocytosis phenotypes of ROM(KD) parasites are two independent features of EhROM1. Whether these two phenotypes are mediated through one or two distinct EhROM1 targets is not known. We have previously demonstrated that the heavy subunit of the Gal/GalNAc lectin is a target for EhROM1, but additional targets could also be present. Rhomboid proteases have been implicated in development, signaling, apoptosis, and host cell entry (3, 11, 49, 53, 58, 60). Thus, roles in adhesion and phagocytosis would both be new functions for rhomboid proteases. Our data represent the first study of a rhomboid protease in an extracellular parasitic pathogen and broaden the potential functional roles played by rhomboid proteases across evolution (16).

The adhesion defect observed in ROM(KD) parasites was unexpected, since we hypothesized that EhROM1 could cleave the Gal/GalNAc lectin, which mediates parasite adhesion to host cells. Thus, EhROM1 downregulation would be postulated to increase surface abundance of the Gal/GalNAc lectin and thus increase parasite adhesion. Interestingly, there were no significant changes in expression or localization of the heavy subunit of the Gal/GalNAc lectin in ROM(KD) parasites. Multiple models can explain the unexpected result of ROM(KD) parasites being less adherent. One possibility is

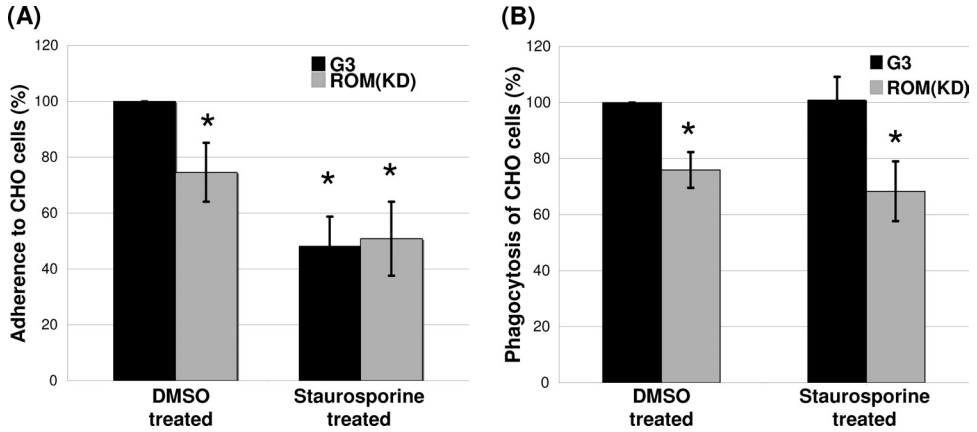

FIG. 7. Adherence to apoptotic treated cells was not reduced in ROM(KD) parasites, but phagocytosis of these cells was decreased. (A) Adherence to staurosporine-treated cells decreased in the parental strain but not in ROM(KD) parasites. CHO cells were treated either with 100 μM staurosporine aglycone or with 100 μM DMSO for 1 h at 4°C, and a CHO cell rosette assay was performed. Data are averages of three independent experiments. Standard deviations are shown. *, $P < 0.002$ for G3 (DMSO treated) versus G3 (staurosporine treated) or $P < 0.003$ for G3 (DMSO treated) versus ROM(KD) (staurosporine treated) cells. (B) Phagocytosis of staurosporine-treated CHO cells was decreased in ROM(KD) parasites. CHO cells were treated with 100 μM staurosporine or with 100 μM DMSO for 1 h at 4°C and subsequently incubated for 15 min at 37°C with parasites (ratio, 1:1). The cells were fixed, permeabilized, and stained with 1% (vol/vol) trichrome stain. Parasites with one or more ingested CHO cells were considered positive for phagocytosis. Data are expressed as the percentage of G3 DMSO-treated levels and are averages of three independent experiments. Standard deviations are shown. *, $P < 0.003$ (DMSO treated) or $P < 0.007$ (staurosporine treated).

that EhROM1 cleaves a substrate on the host cell surface, which requires processing for adhesion. In this scenario EhROM1 would more likely cleave a juxtamembrane site of the host cell surface protein, as it is unlikely that EhROM1 would be able to cleave within the transmembrane domain. Rhomboid proteases have recently been shown to be able to cleave regions outside the transmembrane domain, and so this possibility is feasible (19, 31). A second possibility is that EhROM1 may cleave an unknown substrate on the parasite surface, which masks the Gal/GalNAc lectin under normal conditions. Thus, cleavage and shedding of this surface protein is required in order for the Gal/GalNAc lectin to be accessible to host cells. A third model is that EhROM1, rather than modulating direct attachment between the parasite and host cell, has a role in signaling during the adhesion process. The cytoplasmic domain of Gal/GalNAc lectin contains a β-integrin-like motif, which regulates signaling and plays a role in both adherence and virulence (56). EhROM1-mediated cleavage of the lectin would inhibit inside-out signaling from this domain by severing the attachment between the extracellular and intracellular portions of Hgl. Finally, it is possible that EhROM1 has a noncatalytic role in the adhesion process, as noncatalytic functions of rhomboid proteases have been described previously (26).

ROM(KD) parasites exhibited no alteration in cap formation or complement resistance compared to G3 parasites. One explanation for this is that the small amount of EhROM1 still present in ROM(KD) parasites is able to functionally compensate for these biological processes. Previous biochemical analyses have shown that EhROM1 is a highly active protease (4), so it is possible that despite the very significant downregulation of EhROM1, enough functional protease is still present. Additionally, *E. histolytica* has multiple other means by which it evades the complement cascade, including degradation of components of the membrane attack complex (MAC) by amebic proteases as well as the homology between Hgl and human CD59, which prevents assembly of the MAC on the cell surface (10, 39, 40). Thus, a defect in complement resistance could be masked by compensatory changes in these other mechanisms, which should still be fully functional in ROM(KD) parasites. One final consideration is that the relocalization of EhROM1 to the base of the cap is a passive event. Thus, EhROM1 is excluded from the cap because of its multipass transmembrane architecture and because it does not play significant roles in capping or complement resistance. According to the latest available genome data, *E. histolytica* encodes a single rhomboid protease with the residues required for proteolytic activity. Thus, to the best of our knowledge, no other rhomboid protease exists which could compensate for the loss of function in ROM(KD) parasites. Relocalization of EhROM1 to the base of the cap was most dramatic when the cap appeared to become pinched off for release (4). Further approaches (using live imaging, for example) to study the process of cap release process could provide invaluable data as to whether EhROM1 plays a role in this process.

Our data suggest two distinct roles for EhROM1: in regulating parasite adhesion to viable (but not to apoptotic) host cells and in phagocytosis. The underlying mechanisms behind defects in adhesion and phagocytosis in ROM(KD) parasites are unclear and will require further investigation. In order to further elucidate the role of EhROM1, expression of this gene should be downregulated in a virulent parasite strain in order to examine phenotypes that cannot be measured in G3 parasites. Additionally, whether the Gal/GalNAc lectin is cleaved by EhROM1 in parasites and whether other substrates of EhROM1 exist are important future avenues of investigation.

ACKNOWLEDGMENTS

We are grateful to all members of the Singh and Mirelman labs for their helpful input. We thank Gretchen Ehrenkaufer for help with microarray data and Hussein Alramini with technical assistance. L.B. acknowledges Peter Kao for use of his confocal microscope. We thank W. A. Petri, Jr., for providing the anti-Hgl monoclonal antibodies 3F4, 7F4, and H85.

This work was supported by NIH training grant T32-AI07328 (to L.B.), AI053724 (to U.S.), and a Stanford University Dean's fellowship (to E.R.). The research at the Mirelman lab was supported by a grant from Erica Drake.

REFERENCES

1. **Arhets, P., P. Gounon, P. Sansonetti, and N. Guillen.** 1995. Myosin II is involved in capping and uroid formation in the human pathogen *Entamoeba histolytica*. Infect. Immun. **63:**4358–4367.
2. **Bailey, G. B., D. B. Day, C. Nokkaew, and C. C. Harper.** 1987. Stimulation by target cell membrane lipid of actin polymerization and phagocytosis by *Entamoeba histolytica*. Infect. Immun. **55:**1848–1853.
3. **Baker, R. P., R. Wijetilaka, and S. Urban.** 2006. Two *Plasmodium* rhomboid proteases preferentially cleave different adhesins implicated in all invasive stages of malaria. PLoS Pathog. **2:**e113.
4. **Baxt, L. A., R. P. Baker, U. Singh, and S. Urban.** 2008. An *Entamoeba histolytica* rhomboid protease with atypical specificity cleaves a surface lectin involved in phagocytosis and immune evasion. Genes Dev. **22:**1636–1646.
5. **Belmokhtar, C. A., J. Hillion, and E. Segal-Bendirdjian.** 2001. Staurosporine induces apoptosis through both caspase-dependent and caspase-independent mechanisms. Oncogene **20:**3354–3362.
6. **Bier, E., L. Y. Jan, and Y. N. Jan.** 1990. Rhomboid, a gene required for dorsoventral axis establishment and peripheral nervous system development in *Drosophila melanogaster*. Genes Dev. **4:**190–203.
7. **Boettner, D. R., C. D. Huston, A. S. Linford, S. N. Buss, E. Houpt, N. E. Sherman, and W. A. Petri, Jr.** 2008. *Entamoeba histolytica* phagocytosis of human erythrocytes involves PATMK, a member of the transmembrane kinase family. PLoS Pathog. **4:**e8.
8. **Bracha, R., Y. Nuchamowitz, M. Anbar, and D. Mirelman.** 2006. Transcriptional silencing of multiple genes in trophozoites of *Entamoeba histolytica*. PLoS Pathog. **2:**e48.
9. **Bracha, R., Y. Nuchamowitz, and D. Mirelman.** 2003. Transcriptional silencing of an amoebapore gene in *Entamoeba histolytica*: molecular analysis and effect on pathogenicity. Eukaryot. Cell **2:**295–305.
10. **Braga, L. L., H. Ninomiya, J. J. McCoy, K. Adal, T. Wiedmer, C. Pham, P. J. Sims, and W. A. Petri, Jr.** 1992. Inhibition of the complement membrane attack complex by the galactose-specific adhesin of *Entamoeba histolytica*. Arch. Med. Res. **23:**133.
11. **Brossier, F., T. J. Jewett, L. D. Sibley, and S. Urban.** 2005. A spatially localized rhomboid protease cleaves cell surface adhesins essential for invasion by *Toxoplasma*. Proc. Natl. Acad. Sci. U. S. A. **102:**4146–4151.
12. **Bujanover, S., U. Katz, R. Bracha, and D. Mirelman.** 2003. A virulence attenuated amoebapore-less mutant of *Entamoeba histolytica* and its interaction with host cells. Int. J. Parasitol. **33:**1655–1663.
13. **Calderon, J.** 1980. Dynamic changes on the surface of *Entamoeba* induced by antibodies. Arch. Invest. Med. (Mexico) **11:**55–61.
14. **Calderon, J., and E. E. Avila.** 1986. Antibody-induced caps in *Entamoeba histolytica*: isolation and electrophoretic analysis. J. Infect. Dis. **153:**927–932.
15. **Espinosa-Cantellano, M., and A. Martinez-Palomo.** 1994. *Entamoeba histolytica*: mechanism of surface receptor capping. Exp. Parasitol. **79:**424–435.
16. **Freeman, M.** 2009. Rhomboids: 7 years of a new protease family. Semin. Cell. Dev. Biol. **20:**231–239.
17. **Gilchrist, C. A., D. J. Baba, Y. Zhang, O. Crasta, C. Evans, E. Caler, B. W. Sobral, C. B. Bousquet, M. Leo, A. Hochreiter, S. K. Connell, B. J. Mann, and W. A. Petri.** 2008. Targets of the *Entamoeba histolytica* transcription factor URE3-BP. PLoS Negl. Trop. Dis. **2:**e282.
18. **Gilchrist, C. A., E. Houpt, N. Trapaidze, Z. Fei, O. Crasta, A. Asgharpour, C. Evans, S. Martino-Catt, D. J. Baba, S. Stroup, S. Hamano, G. Ehrenkaufer, M. Okada, U. Singh, T. Nozaki, B. J. Mann, and W. A. Petri, Jr.** 2006. Impact of intestinal colonization and invasion on the *Entamoeba histolytic*a transcriptome. Mol. Biochem. Parasitol. **147:**163–176.
19. **Ha, Y.** 2009. Structure and mechanism of intramembrane protease. Semin. Cell. Dev. Biol. **20:**240–250.

20. **Hamelmann, C., B. Foerster, G. D. Burchard, N. Shetty, and R. D. Horstmann.** 1993. Induction of complement resistance in cloned pathogenic *Entamoeba histolytica*. Parasite Immunol. **15:**223–228.
21. **Hamelmann, C., B. Urban, B. Foerster, and R. D. Horstmann.** 1993. Complement resistance of pathogenic *Entamoeba histolytica* mediated by trypsin-sensitive surface component(s). Infect. Immun. **61:**1636–1640.
22. **Huguenin, M., R. Bracha, T. Chookajorn, and D. Mirelman.** 2010. Epigenetic transcriptional gene silencing in *Entamoeba histolytica*: insight into histone and chromatin modifications. Parasitology **137:**619–627.
23. **Huston, C. D., D. R. Boettner, V. Miller-Sims, and W. A. Petri, Jr.** 2003. Apoptotic killing and phagocytosis of host cells by the parasite *Entamoeba histolytica*. Infect. Immun. **71:**964–972.
24. **Huston, C. D., E. R. Houpt, B. J. Mann, C. S. Hahn, and W. A. Petri, Jr.** 2000. Caspase 3-dependent killing of host cells by the parasite *Entamoeba histolytica*. Cell. Microbiol. **2:**617–625.
25. **Kanaoka, M. M., S. Urban, M. Freeman, and K. Okada.** 2005. An *Arabidopsis* rhomboid homolog is an intramembrane protease in plants. FEBS Lett. **579:**5723–5728.
26. **Karakasis, K., D. Taylor, and K. Ko.** 2007. Uncovering a link between a plastid translocon component and rhomboid proteases using yeast mitochondria-based assays. Plant Cell Physiol. **48:**655–661.
27. **Labruyere, E., and N. Guillen.** 2006. Host tissue invasion by *Entamoeba histolytica* is powered by motility and phagocytosis. Arch. Med. Res. **37:**253–258.
28. **Lemberg, M. K., and M. Freeman.** 2007. Cutting proteins within lipid bilayers: rhomboid structure and mechanism. Mol. Cell **28:**930–940.
29. **MacFarlane, R. C., and U. Singh.** 2006. Identification of differentially expressed genes in virulent and nonvirulent *Entamoeba* species: potential implications for amebic pathogenesis. Infect. Immun. **74:**340–351.
30. **MacFarlane, R. C., and U. Singh.** 2007. Identification of an *Entamoeba histolytica* serine-, threonine-, and isoleucine-rich protein with roles in adhesion and cytotoxicity. Eukaryot. Cell **6:**2139–2146.
31. **Maegawa, S., K. Koide, K. Ito, and Y. Akiyama.** 2007. The intramembrane active site of GlpG, an *E. coli* rhomboid protease, is accessible to water and hydrolyses an extramembrane peptide bond of substrates. Mol. Microbiol. **64:**435–447.
32. **Mayer, U., and C. Nusslein-Volhard.** 1988. A group of genes required for pattern formation in the ventral ectoderm of the *Drosophila* embryo. Genes Dev. **2:**1496–1511.
33. **McQuibban, G. A., S. Saurya, and M. Freeman.** 2003. Mitochondrial membrane remodelling regulated by a conserved rhomboid protease. Nature **423:**537–541.
34. **Mora-Galindo, J., M. Gutierrez-Lozano, and F. Anaya-Velazquez.** 1997. *Entamoeba histolytica*: kinetics of hemolytic activity, erythrophagocytosis and digestion of erythrocytes. Arch. Med. Res. **28**(Spec. issue)**:**200–201.
35. **Pascall, J. C., and K. D. Brown.** 2004. Intramembrane cleavage of ephrinB3 by the human rhomboid family protease, RHBDL2. Biochem. Biophys. Res. Commun. **317:**244–252.
36. **Petri, W. A., Jr., R. D. Smith, P. H. Schlesinger, C. F. Murphy, and J. I. Ravdin.** 1987. Isolation of the galactose-binding lectin that mediates the in vitro adherence of *Entamoeba histolytica*. J. Clin. Invest. **80:**1238–1244.
37. **Que, X., and S. L. Reed.** 1997. The role of extracellular cysteine proteinases in pathogenesis of *Entamoeba histolytica* invasion. Parasitol. Today **13:**190–194.
38. **Ravdin, J. I., C. F. Murphy, R. A. Salata, R. L. Guerrant, and E. L. Hewlett.** 1985. *N*-Acetyl-D-galactosamine-inhibitable adherence lectin of *Entamoeba histolytica*. I. Partial purification and relation to amoebic virulence in vitro. J. Infect. Dis. **151:**804–815.
39. **Reed, S. L., J. A. Ember, D. S. Herdman, R. G. DiScipio, T. E. Hugli, and I. Gigli.** 1995. The extracellular neutral cysteine proteinase of *Entamoeba histolytica* degrades anaphylatoxins C3a and C5a. J. Immunol. **155:**266–274.
40. **Reed, S. L., W. E. Keene, J. H. McKerrow, and I. Gigli.** 1989. Cleavage of C3 by a neutral cysteine proteinase of *Entamoeba histolytica*. J. Immunol. **143:**189–195.
41. **Rosenberg, I., D. Bach, L. M. Loew, and C. Gitler.** 1989. Isolation, characterization and partial purification of a transferable membrane channel (amoebapore) produced by *Entamoeba histolytica*. Mol. Biochem. Parasitol. **33:**237–247.
42. **Saffer, L. D., and W. A. Petri, Jr.** 1991. Role of the galactose lectin of *Entamoeba histolytica* in adherence-dependent killing of mammalian cells. Infect. Immun. **59:**4681–4683.
43. **Saito-Nakano, Y., T. Yasuda, K. Nakada-Tsukui, M. Leippe, and T. Nozaki.** 2004. Rab5-associated vacuoles play a unique role in phagocytosis of the enteric protozoan parasite *Entamoeba histolytica*. J. Biol. Chem. **279:**49497–49507.
44. **Segal-Bendirdjian, E., and A. Jacquemin-Sablon.** 1995. Cisplatin resistance in a murine leukemia cell line is associated with a defective apoptotic process. Exp. Cell Res. **218:**201–212.
45. **Silva, P. P., A. Martinez-Palomo, and A. Gonzalez-Robles.** 1975. Membrane structure and surface coat of *Entamoeba histolytica.* Topochemistry and dynamics of the cell surface: cap formation and microexudate. J. Cell Biol. **64:**538–550.
46. **Singh, S., M. Plassmeyer, D. Gaur, and L. H. Miller.** 2007. Mononeme: a new secretory organelle in *Plasmodium falciparum* merozoites identified by localization of rhomboid-1 protease. Proc. Natl. Acad. Sci. U. S. A. **104:**20043–20048.
47. **Srinivasan, P., I. Coppens, and M. Jacobs-Lorena.** 2009. Distinct roles of *Plasmodium* rhomboid 1 in parasite development and malaria pathogenesis. PLoS Pathog. **5:**e1000262.
48. **Stauffer, W., and J. I. Ravdin.** 2003. *Entamoeba histolytica*: an update. Curr. Opin. Infect. Dis. **16:**479–485.
49. **Stevenson, L. G., K. Strisovsky, K. M. Clemmer, S. Bhatt, M. Freeman, and P. N. Rather.** 2007. Rhomboid protease AarA mediates quorum-sensing in *Providencia stuartii* by activating TatA of the twin-arginine translocase. Proc. Natl. Acad. Sci. U. S. A. **104:**1003–1008.
50. **Teixeira, J. E., and C. D. Huston.** 2008. Participation of the serine-rich *Entamoeba histolytica* protein in amebic phagocytosis of apoptotic host cells. Infect. Immun. **76:**959–966.
51. **Trissl, D., A. Martinez-Palomo, M. de la Torre, R. de la Hoz, and E. Perez de Suarez.** 1978. Surface properties of *Entamoeba*: increased rates of human erythrocyte phagocytosis in pathogenic strains. J. Exp. Med. **148:**1137–1143.
52. **Urban, S., and M. Freeman.** 2003. Substrate specificity of rhomboid intramembrane proteases is governed by helix-breaking residues in the substrate transmembrane domain. Mol. Cell **11:**1425–1434.
53. **Urban, S., J. R. Lee, and M. Freeman.** 2001. *Drosophila* rhomboid-1 defines a family of putative intramembrane serine proteases. Cell **107:**173–182.
54. **Urban, S., J. R. Lee, and M. Freeman.** 2002. A family of rhomboid intramembrane proteases activates all *Drosophila* membrane-tethered EGF ligands. EMBO J. **21:**4277–4286.
55. **Urban, S., and M. S. Wolfe.** 2005. Reconstitution of intramembrane proteolysis in vitro reveals that pure rhomboid is sufficient for catalysis and specificity. Proc. Natl. Acad. Sci. U. S. A. **102:**1883–1888.
56. **Vines, R. R., G. Ramakrishnan, J. B. Rogers, L. A. Lockhart, B. J. Mann, and W. A. Petri, Jr.** 1998. Regulation of adherence and virulence by the *Entamoeba histolytica* lectin cytoplasmic domain, which contains a β2 integrin motif. Mol. Biol. Cell **9:**2069–2079.
57. **Voigt, H., and N. Guillen.** 1999. New insights into the role of the cytoskeleton in phagocytosis of *Entamoeba histolytica*. Cell. Microbiol. **1:**195–203.
58. **Wang, Y., X. Guan, K. L. Fok, S. Li, X. Zhang, S. Miao, S. Zong, S. S. Koide, H. C. Chan, and L. Wang.** 2008. A novel member of the Rhomboid family, RHBDD1, regulates BIK-mediated apoptosis. Cell. Mol. Life Sci. **65:**3822–3829.
59. **Wasserman, J. D., S. Urban, and M. Freeman.** 2000. A family of rhomboid-like genes: *Drosophila* rhomboid-1 and roughoid/rhomboid-3 cooperate to activate EGF receptor signaling. Genes Dev. **14:**1651–1663.
60. **Yan, Z., H. Zou, F. Tian, J. R. Grandis, A. J. Mixson, P. Y. Lu, and L. Y. Li.** 2008. Human rhomboid family 1 gene silencing causes apoptosis or autophagy to epithelial cancer cells and inhibits xenograft tumor growth. Mol. Cancer Ther. **7:**1355–1364.